Lecture 7
Transition Scenarios: Normality vs Non-Normality

Lecturer: Rich Kerswell.
Write-up: Giulio Mariotti and Lindsey Ritchie

June 28, 2011

1 Transition scenarios

Transition to turbulence in fluid systems can be broadly divided into two different classes: the 'supercritical' or the 'subcritical' scenario.

1.1 Supercritical scenario

In the supercritical scenario, there is a well-defined sequence of supercritical bifurcations in which the flow gradually becomes more complicated in space and time. For these flows, nothing happens (that is, all disturbances decay) below a well-defined value of a control parameter, e.g. the Reynolds number Re. The following commonly-referred-to values of the control parameter R (e.g. [19]) then effectively characterise the situation:

- R_E, the threshold below which any disturbances, both finite and infinitesimal, monotonically decay. This is known as the Energy stability threshold.
- R_L, the threshold for linear stability.
- R_G, the least R below which the basin of attraction of the laminar solution includes all states with the exception of a set of states of measure zero. R_G signals the emergence of another attractor beyond the laminar solution.

In the supercritical scenario where the first bifurcation from the base state is supercritical, $R_E \leq R_L = R_G$. The only interesting issue is then whether $R_E = R_L$ or $R_E < R_L$ so there is a gap.

Rayleigh-Bénard convection (RB) is an example of a flow in the supercritical scenario class (e.g. see [6], chapter 6). The motionless conductive state is provably absolutely stable (i.e. to *all* disturbances) until a certain value ($Ra_L = 1708$ for rigid-rigid boundary conditions, where Ra is the Rayleigh number) so $R_E = R_L = R_G = 1708$. Above this value, the flow undergoes a sequence of supercritical bifurcations.

Another member of the supercritical scenario class is Taylor-Couette flow (TC) with co-rotating cylinders. TC flow shows a succession of bifurcations and increasing complexity for $R := R_i > R_L > 0$ (increasing rotation rate of the inner cylinder and fixed outer cylinder rotation rate $R_o > 0$): see figure 1. Contrary to RB flow, $R_E < R_L = R_G$ which means that

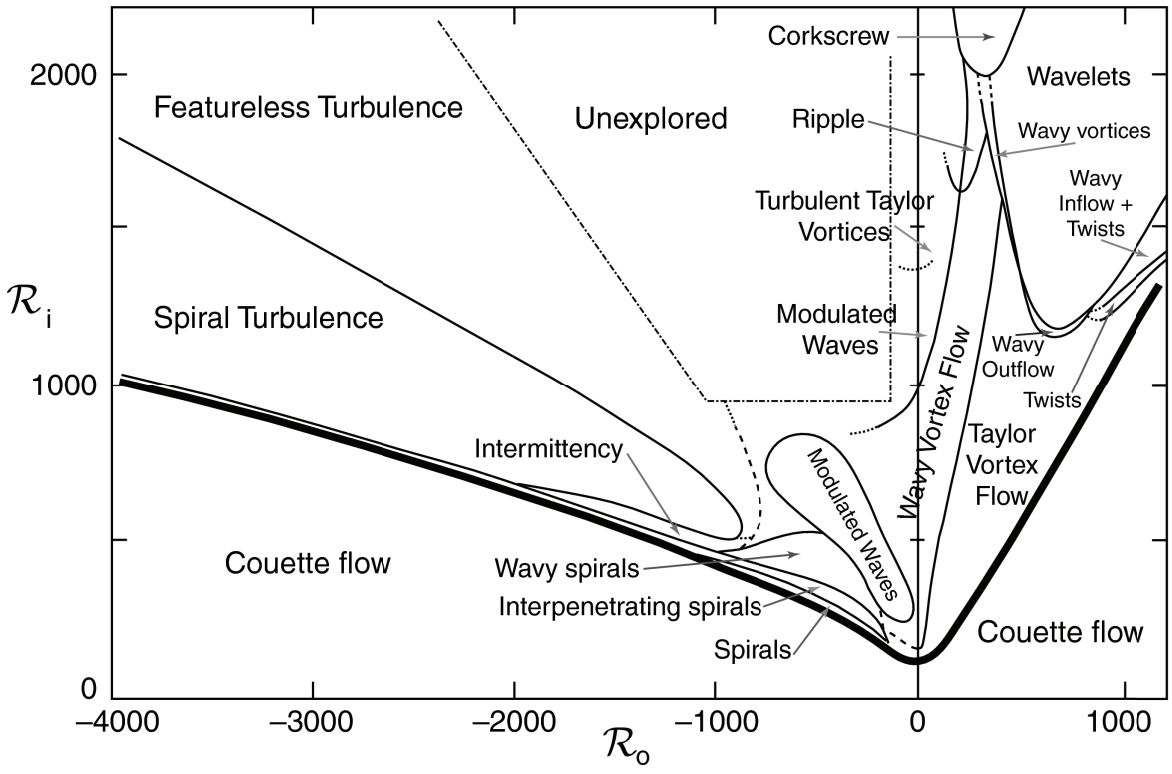

Figure 1: Phase diagram of patterns observed in Taylor-Couette flow as a function of the inner Reynolds number R_i and the outer Reynolds number R_o. The heavy line denotes the boundary between featureless flow below the line and patterned states above the line. (Redrawn from [1], see also [6], figure 7.8).

transient growth - an initial disturbance can initially grow in amplitude before eventually decaying away - is possible for $R_E < R < R_L$ with TC flow (see figure 2). The supercritical scenario is well-studied and understood.

1.2 Subcritical scenarios

In the subcritical scenario, as typified by wall-bounded shear flows, transition is sudden, noise-dependent and dramatic, i.e. the flow immediately becomes complicated. There is usually a region of bistability so that the laminar and turbulent states can coexist (in plane Couette and Hagen-Poiseuille flow, this region extends to infinite Re!). As a result this is the more interesting scenario where there has been considerable recent research activity and so will be the focus of my lectures. Flows in the subcritical scenario class cannot be sufficiently described by the three (established) parameters defined above. Therefore, as a first attempt in building up a more sophisticated picture, we introduce the following additional parameter values:

- R_S, the threshold above which there exists initial conditions with measure zero which do not convergence to the basic state. Or equivalently, there exists 'other' unstable

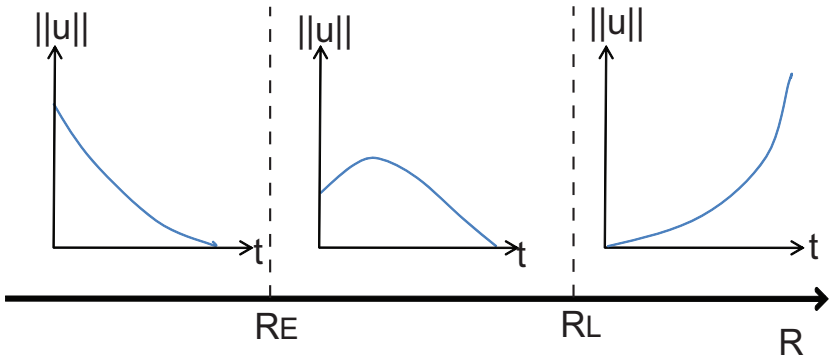

Figure 2: Sketch of different solution characteristics under different values of R for the supercritical scenario.

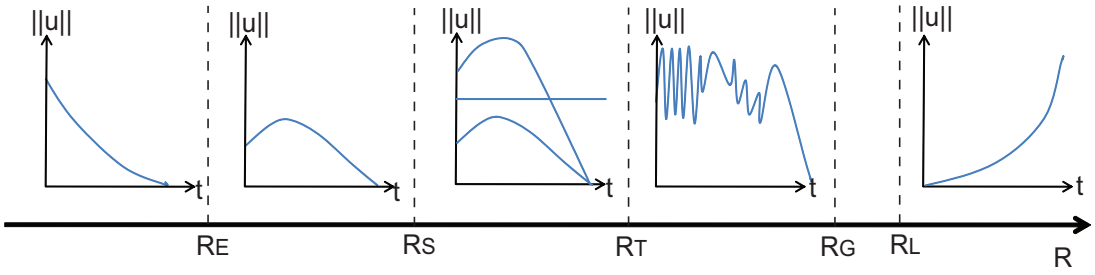

Figure 3: Sketch of different solution characteristics under different values of R for the subcritical scenario.

exact solutions of the governing equations beyond the basic state.

- R_T, the threshold above which long-lived non-trivial flows exist. These flows look turbulent (characterised by positive Lyapunov exponents so nearby trajectories diverge) but may not be sustained if $R_T < R < R_G$.

For subcritical scenarios we have that $R_E < R_S, R_T \leq R_G$, where $R_S < R_T$ seems likely but is unproven and typically $R_G < R_L$ for wall-bounded shear flows like plane Poiseuille flow, plane Couette flow and Hagen-Poiseuille flow. The qualitative behaviour of a typical subcritical scenario is sketched in figure 3. For $R < R_E$ all solutions decay monotonically to the base state. For $R_E < R < R_S$ transient growth is possible of some disturbances. For $R_S < R < R_T$ at least one disturbance does not decay to the base state. For $R_T < R < R_G$ at least one solution experiences a 'long-lived' transient before eventually decaying. For $R_G < R < R_L$ the flow need not relaminarise when disturbed and finally, for $R > R_L$ the flow always evolves away from the base state. Table 1 emphasizes how the Rayleigh-Bénard problem differs from plane Poiseuille, plane Couette and Hagen-Poiseuille flows which are all in the subcritical scenario class.

	R_E	R_S	R_T	R_L
RB	$1708^{[8]}$	1708	1708	1708
PPF	$49.6^{[4]}$	$\leq 977^{+[20]}$	$2100^{[18]}$	$5772^{[13]}$
PCF	$20.7^{[8]}$	$\leq 127^{[12,\ 20]}$	$\sim 325^{[5]}$	$\infty^{[17]}$
HPF	$81.5^{[9]}$	$\leq 773^{*[15]}$	$\sim 1800^{[11]}$	$\infty^{\dagger}$

Table 1: The various thresholds for different flow types: Rayleigh-Bénard (RB), plane Poiseuille flow (PPF), plane Couette flow (PCF), and Hagen-Poiseuille flow (HPF). Source references are shown as superscripts and † indicates still unproven. $^{+}$ means R_S is based upon fixed pressure gradient whereas * means R_S based upon fixed mass flux. R_S for PPF based upon fixed mass flux is close to but strictly below 860 whereas HPF based upon pressure gradient is close to, but strictly below, 990.

1.3 Normality vs Non-normality

We now discuss the reasons for this very different behaviour which, because of the special form of the nonlinearity in the Navier-Stokes equation, can be largely traced back to the properties of the linear operator produced by linearising the Navier-Stokes equation around the basic state.

If $\mathbf{u}_{\rm tot} = \mathbf{u}_{\rm lam} + \hat{\mathbf{u}}$ so $\hat{\mathbf{u}}$ satisfies homogeneous boundary conditions (is real, at least C^2 and has finite kinetic energy), then the Navier-Stokes equation for the perturbation $\hat{\mathbf{u}}$ can be written as

$$\frac{\partial \hat{\mathbf{u}}}{\partial t} = L\hat{\mathbf{u}} + N(\hat{\mathbf{u}}, \hat{\mathbf{u}}), \tag{1}$$

$$\nabla \cdot \hat{\mathbf{u}} = 0, \tag{2}$$

where L and N are linear and nonlinear operators, respectively. If $\langle \mathbf{u}, \mathbf{v} \rangle := \int \mathbf{u}^*.\mathbf{v}\, dV$ where * indicates complex conjugation (redundant here for real $\hat{\mathbf{u}}$ but important when discussing the eigenfunctions and adjoint of L), then

$$\left\langle (L^+\mathbf{u}), \mathbf{v} \right\rangle := \langle \mathbf{u}, (L\mathbf{v}) \rangle \tag{3}$$

defines L^+, the adjoint of L and L is normal if and only if L^+ commutes with L i.e. $LL^+ = L^+L$. The eigenvalue spectrum of the linear operator L determines the linear stability of the base state $\mathbf{u}_{\rm lam}$ with R_L defined by when $\max[\Re e(\mathrm{eig}(L))] = 0$. Energy stability is derived by examining the instantaneous rate of change of the perturbation kinetic energy,

$$\frac{\partial}{\partial t}\langle \frac{1}{2}\hat{\mathbf{u}}^2 \rangle = \left\langle \hat{\mathbf{u}}, \frac{\partial \hat{\mathbf{u}}}{\partial t} \right\rangle = \langle \hat{\mathbf{u}}, (L\hat{\mathbf{u}}) \rangle = \tfrac{1}{2} \left\langle \hat{\mathbf{u}}, (L + L^+)\hat{\mathbf{u}} \right\rangle \tag{4}$$

since $\langle \hat{\mathbf{u}}, N(\hat{\mathbf{u}}, \hat{\mathbf{u}}) \rangle = 0$ (this is the special property of the Navier-Stokes equations referred to immediately above) and L can always be decomposed into 'symmetric' and 'antisymmetric' parts, $L = \frac{1}{2}(L+L^+)+\frac{1}{2}(L-L^+)$. Clearly there can only be energy growth if the right hand side of (4) is positive for at least one allowable $\hat{\mathbf{u}}$ (where 'allowable' is taken to mean a real incompressible velocity field which is twice-differentiable, satisfies the boundary conditions and has finite kinetic energy). Since $L + L^+$ is a self-adjoint (symmetric) operator, this can only happen if one of its eigenvalues is positive (recall all eigenvalues of a self-adjoint operator are real). If L is self-adjoint, then this is one and the same condition that the flow is linearly unstable so $R_E = R_L$. However, the weaker condition that L is normal is also sufficient. This is because if L has the (possibly complex) eigenvalue and eigenfunction pair $(\mu_i, \mathbf{v}_i)$ then L^+ has the equivalent pair $(\mu_i^*, \mathbf{v}_i)$ when L commutes with L^+. Then

$$\mathrm{eig}(\, \tfrac{1}{2}(L + L^+)\,) = \Re e(\, \mathrm{eig}(L)\,) \tag{5}$$

and so energy growth starts to occur precisely when an eigenvalue of L crosses into the right hand side of the complex plane. Hence

$$\text{Normality of } \; L \Rightarrow R_E = R_L \Rightarrow \text{supercriticality.} \tag{6}$$

The bifurcation at R_L has to be supercritical as the laminar state is the global attractor for $R < R_E$. The reverse direction is not valid, i.e. supercriticality does *not* imply $R_E = R_L$ as we will see in the example of rotating plane Couette flow below.

A subcritical bifurcation at R_L implies $R_E < R_L$ and therefore the possibility of transient growth: for some (but not all) $\hat{\mathbf{u}}$, the perturbation energy will initially grow but ultimately decay for $R_E < R < R_L$. This means that an eigenvalue of $L + L^+$ must reach into the right hand side of the complex plane while no eigenvalue of L does so L has to be non-normal. In other words

$$\text{Non-Normality of } \; L \Leftarrow R_E < R_L \Leftarrow \text{subcriticality.} \tag{7}$$

The arrows cannot be reversed as non-normality does not imply $R_E < R_L$. It is theoretically possible (but presumably unusual) to have a non-normal operator where the largest eigenvalue of $(L + L^+)$ becomes positive precisely when the eigenvalue of largest real part for L crosses onto the right hand side of the complex plane. From a different perspective, non-normality of L implies that the eigenfunctions of L are non-orthogonal but this in itself is not sufficient to produce transient growth as the following example illustrates. Let $\mathbf{u} = \mathbf{v}e^{\lambda_1 t} + \mathbf{w}e^{\lambda_2 t}$ where λ_1 and λ_2 are negative and $\mathbf{v}.\mathbf{w} \neq 0$. If $\mathbf{v}^2 = c_1^2$, $\mathbf{w}^2 = c_2^2$, $\mathbf{v}.\mathbf{w} = \alpha c_1 c_2$ where $0 < \alpha^2 < 1$ and $\mathbf{c} = (c_1 \quad c_2)^T$, then

$$\frac{d\mathbf{u}^2}{dt}|_{t=0} = \mathbf{c}^T\mathbf{B}\mathbf{c} \quad \text{where} \quad \mathbf{B} := \begin{bmatrix} 2\lambda_1 & \alpha(\lambda_1+\lambda_2) \\ \alpha(\lambda_1+\lambda_2) & 2\lambda_2 \end{bmatrix}. \tag{8}$$

For no transient growth, $\mathbf{B}$ must be negative definite. Since $\mathbf{B}$ is symmetric this requires both of its eigenvalues to be negative which is the condition that $4\lambda_1\lambda_2 > \alpha^2(\lambda_1+\lambda_2)^2$. This can always be achieved by choosing α small enough (thanks to Divakar Viswanath for this nice example).

So, in summary, if the linear operator is normal then $R_E = R_L$, otherwise the operator is non-normal which is a necessary but not sufficient condition for a subcritical bifurcation.

1.4 Transient growth

To illustrate the phenomenon of transient growth we consider a simple system of 2 ODEs given by

$$\frac{\mathrm{d}}{\mathrm{d}t}\begin{bmatrix} x(t) \\ \\ y(t) \end{bmatrix} = A\mathbf{x}(t) = \begin{bmatrix} -\dfrac{1}{Re} & 0 \\ 1 & -\dfrac{2}{Re} \end{bmatrix} \begin{bmatrix} x(t) \\ \\ y(t) \end{bmatrix} \tag{9}$$

where x represents rolls and y streaks (say). The operator A is non-normal since $AA^T \neq A^TA$ (transpose being the matrix equivalent of adjoint) and has eigenvalues $-1/Re$ and $-2/Re$. The initial rate of change of the 'energy' is

$$\frac{d}{dt}\mathbf{x}^2 = \mathbf{x}^T\left(A + A^T\right)\mathbf{x} \tag{10}$$

Since $A+A^T$ is symmetric, all that is needed to find initial growth is a positive eigenvalue and initial conditions with sufficient overlap with the corresponding eigendirection. The simple initial conditions $x(0) = y(0) = 1$ are adequate (providing $Re > 3$) since the solution,

$$\begin{bmatrix} x(t) \\ \\ y(t) \end{bmatrix} = \begin{bmatrix} 1 \\ \\ Re \end{bmatrix} e^{-t/Re} + \begin{bmatrix} 0 \\ \\ 1-Re \end{bmatrix} e^{-2t/Re} \sim \begin{bmatrix} 1 - \frac{t}{Re} + \mathcal{O}\left(\frac{t^2}{Re^2}\right) \\ 1 + \frac{Re-2}{Re}t + \mathcal{O}\left(\frac{t^2}{Re^2}\right) \end{bmatrix}, \tag{11}$$

has the initial energy behaviour

$$E(t) := \frac{1}{2}(x^2(t) + y^2(t)) = 1 + \frac{(Re-3)}{Re}t + \mathcal{O}\left(\frac{t^2}{Re^2}\right) \tag{12}$$

Although the rolls decay, there is enough initial growth in the streaks to give overall energy growth even though both eigenvalues of the system are negative.

2 Bifurcation Analysis

In wall-bounded shear flows, the linear operator is generically non-normal and therefore to understand the situation we need to find other nonlinear solutions which exist. There are a variety of methods that can be used, but the first (default) way is to use bifurcation analysis and nonlinear branch continuation techniques. Rotating plane Couette flow presents a beautifully accessible arena in which to illustrate this while also indicating how the first nonlinear solutions in plane Couette flow were found by Nagata [12]. The governing Navier-Stokes equations for an incompressible flow are

$$\frac{\partial \mathbf{u}_{\mathrm{tot}}}{\partial t} + 2\Omega\hat{\mathbf{z}} \times \mathbf{u}_{\mathrm{tot}} + \mathbf{u}_{\mathrm{tot}} \cdot \nabla \mathbf{u}_{\mathrm{tot}} + \nabla p = \frac{1}{Re}\nabla^2 \mathbf{u}_{\mathrm{tot}}, \tag{13}$$

$$\nabla \cdot \mathbf{u}_{\mathrm{tot}} = 0, \tag{14}$$

where $\mathbf{u}_{\mathrm{tot}}(x, \pm 1, z, t) = \pm\hat{\mathbf{x}}$ and $\boldsymbol{\Omega} = \Omega\hat{\mathbf{z}}$ is the spanwise rotation rate. As in §1.3, we define $\mathbf{u}_{\mathrm{tot}} = \mathbf{u}_{\mathrm{lam}} + \hat{\mathbf{u}}$, where $\hat{\mathbf{u}} := (\hat{u}, \hat{v}, \hat{w})$ is a (possibly large) perturbation to the laminar base

state $\mathbf{u}_{\rm lam} := y\hat{\mathbf{x}}$ so that the full perturbation equations are

$$\frac{\partial \hat{\mathbf{u}}}{\partial t} + 2\Omega\hat{\mathbf{z}} \times \hat{\mathbf{u}} + \mathbf{u}_{\rm lam} \cdot \nabla\hat{\mathbf{u}} + \hat{\mathbf{u}} \cdot \nabla\mathbf{u}_{\rm lam} + \hat{\mathbf{u}} \cdot \nabla\hat{\mathbf{u}} + \nabla\hat{p} = \frac{1}{Re}\nabla^2\hat{\mathbf{u}}, \tag{15}$$

$$\nabla \cdot \hat{\mathbf{u}} = 0, \tag{16}$$

where now $\hat{\mathbf{u}}(x, \pm 1, z, t) = \mathbf{0}$. Firstly, we compare the energy and linear stability thresholds for this problem.

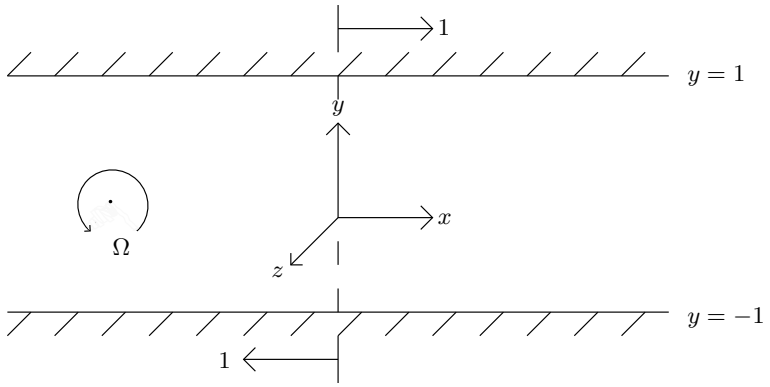

Figure 4: (Spanwise) Rotating Plane Couette flow

2.1 Energy stability

The energy equation is derived by taking the scalar product of $\hat{\mathbf{u}}$ with (15),

$$\begin{aligned}\langle \hat{\mathbf{u}} \cdot (15)\rangle = \frac{\partial}{\partial t}\langle \frac{1}{2}\hat{\mathbf{u}}^2\rangle = &- \langle 2\Omega\hat{\mathbf{z}} \times \hat{\mathbf{u}} \cdot \hat{\mathbf{u}}\rangle - \langle \mathbf{u}_{\rm lam} \cdot \nabla\frac{1}{2}\hat{\mathbf{u}}^2\rangle - \langle \hat{\mathbf{u}} \cdot \hat{\mathbf{u}} \cdot \nabla\hat{\mathbf{u}}\rangle \\ &- \langle \hat{\mathbf{u}} \cdot \nabla\mathbf{u}_{\rm lam} \cdot \hat{\mathbf{u}}\rangle - \langle \hat{\mathbf{u}} \cdot \nabla\hat{p}\rangle - \frac{1}{Re}\langle |\nabla\hat{\mathbf{u}}|^2\rangle,\end{aligned} \tag{17}$$

(where

$$\langle (\ldots)\rangle := \int\int\int (\ldots) \mathrm{d}V = \lim_{L_x\to\infty}\lim_{L_z\to\infty} \frac{1}{4L_xL_z}\int_{-L_x}^{L_x}\int_{-L_z}^{L_z}\int_{-1}^{1} (\ldots)\mathrm{d}y\mathrm{d}z\mathrm{d}x \quad) \tag{18}$$

which simplifies to

$$\begin{aligned}\frac{\partial E}{\partial t} &= -\langle \hat{\mathbf{u}} \cdot \nabla\mathbf{u}_{\rm lam} \cdot \hat{\mathbf{u}}\rangle - \frac{1}{Re}\langle |\nabla\hat{\mathbf{u}}|^2\rangle \\ &= \langle |\nabla\hat{\mathbf{u}}|^2\rangle \left[-\frac{\langle \hat{\mathbf{u}} \cdot \nabla\mathbf{u}_{\rm lam} \cdot \hat{\mathbf{u}}\rangle}{\langle |\nabla\hat{\mathbf{u}}|^2\rangle} - \frac{1}{Re}\right].\end{aligned} \tag{19}$$

Hence, energy growth is possible only if $-\langle \hat{\mathbf{u}} \cdot \nabla\mathbf{u}_{\rm lam} \cdot \hat{\mathbf{u}}\rangle > \frac{1}{Re}\langle |\nabla\hat{\mathbf{u}}|^2\rangle$ or, turning this around, there is a threshold Re_E defined as

$$\frac{1}{Re_E} \equiv \max_{\nabla.\hat{\mathbf{u}}=0, \hat{\mathbf{u}}(x,\pm1,z,t)=\mathbf{0}} \frac{-\langle \hat{\mathbf{u}} \cdot \nabla\mathbf{u}_{\rm lam} \cdot \hat{\mathbf{u}}\rangle}{\langle |\nabla\hat{\mathbf{u}}|^2\rangle} \tag{20}$$

below which no energy growth is possible. After some manipulation, the eigenvalue problem for Re_E can be written as

$$\frac{1}{2}\left[\nabla \mathbf{u}_{\text{lam}} + (\nabla \mathbf{u}_{\text{lam}})^T\right] \cdot \hat{\mathbf{u}} + \nabla \hat{p} = \frac{1}{Re_E}\nabla^2 \hat{\mathbf{u}}, \tag{21}$$

which, since $\mathbf{u}_{\text{lam}} = y\hat{\mathbf{x}}$, simplifies to

$$\frac{1}{2}\begin{bmatrix}\hat{v}\\ \hat{u}\\ 0\end{bmatrix} + \nabla \hat{p} = \frac{1}{Re_E}\nabla^2 \hat{\mathbf{u}} \tag{22}$$

together with $\nabla.\hat{\mathbf{u}} = 0$ and $\hat{\mathbf{u}}(x, \pm 1, z) = \mathbf{0}$.

2.2 Linear stability

Linearising equation (15) gives

$$\frac{\partial \hat{\mathbf{u}}}{\partial t} + 2\Omega\hat{\mathbf{z}} \times \hat{\mathbf{u}} + \mathbf{u}_{\text{lam}} \cdot \nabla \hat{\mathbf{u}} + \hat{\mathbf{u}} \cdot \nabla \mathbf{u}_{\text{lam}} + \nabla \hat{p} = \frac{1}{Re}\nabla^2 \hat{\mathbf{u}}. \tag{23}$$

Assuming streamwise Taylor (2D) roll solutions of the form

$$\hat{\mathbf{u}}(\mathbf{x}, t) = \tilde{\mathbf{u}}(y)e^{ikz+\sigma t} \tag{24}$$

(known to be critical for the energy stability problem), (23) becomes

$$\sigma\tilde{\mathbf{u}} + \begin{bmatrix}(1-2\Omega)\tilde{v}\\ 2\Omega\tilde{u}\\ 0\end{bmatrix} + \nabla \tilde{p} = \frac{1}{Re}\nabla^2 \tilde{\mathbf{u}}. \tag{25}$$

Comparing equation (25) to the energy stability equation (22) we see that when $\Omega = 1/4$, the operators from the energy and linear stability are identical providing $\sigma = 0$ also. This is a special case of a more general relationship between Re_E and Re_L which can be extracted by reducing (25) down to a problem in just $\tilde{v}$. Eliminating $\hat{w}$ using the incompressibility condition, $\hat{p}$ from $\hat{\mathbf{z}}.(25)$ and $\hat{u}$ from $\hat{\mathbf{x}}.(25)$ leaves

$$2Re^2\Omega(1-2\Omega)k^2\tilde{v} = -(D^2 - k^2 - \sigma Re)^2(D^2 - k^2)\tilde{v}, \tag{26}$$

to be solved subject to boundary conditions

$$\tilde{v} = D\tilde{v} = (D^2 - k^2 - \sigma Re)(D^2 - k^2)\tilde{v} = 0 \text{ at } y = \pm 1, \tag{27}$$

where $D := \mathrm{d}/\mathrm{d}y$. This system must be solved to find $Re_L = \min_k Re$ such that $\Re e(\sigma) = 0$. Conveniently, this can be done by comparing it to the Rayleigh-Bénard convection problem given by

$$k^2 Ra\,\tilde{w} = -(D^2 - k^2 - \sigma)^2(D^2 - k^2)\tilde{w} \tag{28}$$

with boundary conditions

$$\tilde{w} = D\tilde{w} = (D^2 - k^2 - \sigma)(D^2 - k^2)\tilde{w} = 0 \text{ at } y = \pm\frac{1}{2}, \tag{29}$$

where Ra is the Rayleigh number. This system has a well-known solution, with $\min_k Ra = 1708$ for $\sigma = 0$ and $k = 3.117$ (Drazin 2002, section 6.3 and the rigid-rigid case). Since the layer depth for Rayleigh-Bénard convection is standardly non-dimensionalised to be 1 whereas it is 2 here (e.g. compare positions of boundaries), the lengths in equations (26) and (27) need to be rescaled to make the connection exact. Letting $D^2 \to \frac{1}{4}D^2$, $k^2 \to \frac{1}{4}k^2$ and setting $\sigma = 0$ means the association

$$Re_L^2 = \frac{1708}{2^4[2\Omega(1-2\Omega)]} \tag{30}$$

can be made. The minimum of Re_L occurs when $\Omega = 1/4$ (as noticed above) where the linear operator is normal and so

$$\min_{k,\Omega} Re_L = 20.67 = Re_E. \tag{31}$$

More generally ($\Omega \neq 1/4$)

$$Re_L = \frac{Re_E}{\sqrt{8\Omega(1-2\Omega)}} \tag{32}$$

exceeds Re_E and the linear operator is non-normal. Notice also that $Re_L \to \infty$ for $\Omega \to 0$ and $1/2$. Beyond these values, there is no linear instability: the Rayleigh number in the analogous Rayleigh-Benard problem is then negative indicating that the stationary fluid is now hotter on its top surface than the bottom which is a very stable situation.

Figure 5 shows the bifurcation diagram for rotating plane Couette flow. The 2-dimensional steady solution surface emanating out of the bifurcation given by (32) is shown in blue. This is traced out by considering the velocity expansion

$$\begin{bmatrix} \mathbf{u}(y,z) \\ p(y,z) \end{bmatrix} = \sum_{l=-\infty}^{+\infty} \begin{bmatrix} \tilde{\mathbf{u}}_l(y) \\ \tilde{p}_l(y) \end{bmatrix} e^{ilkz} \tag{33}$$

truncated to some finite positive upper and negative lower values in l where k is the critical wavenumber (a weakly nonlinear solution would just have $l = 0, \pm 1, \pm 2$ only). The expansion functions $\tilde{\mathbf{u}}_l(y)$ and $\tilde{p}_l$ are typically themselves expanded in terms of basis functions in y so that the solution is represented by a doubly-indexed set of complex coefficients. Solutions are then found using root-finding algorithms invariably based upon the Newton-Raphson method. These 2D solutions become unstable to 3D steady disturbances (shown as a green curve). By tracing these solutions around in (Re, Ω) parameter space, Nagata [12] found that they pierced the $\Omega = 0$ plane for $Re \geq 125$ (later more accurately computed to be 127.7 [20]). These non-rotating steady 3D solutions (shown in red) were the first discovery of exact solutions to plane Couette flow beyond the simple constant shear state.

The rotating plane Couette system is also of interest in astrophysics for studying the fluid dynamics of accretion disks (e.g. [16]). A disk with an angular velocity profile of $\Omega^* \sim R^{-q}$ and a thin distant radial strip $R \in [R-1, R+1]$ (with $1 \ll R$) looks locally like rotating PCF with

$$\Omega = \frac{1}{q} \tag{34}$$

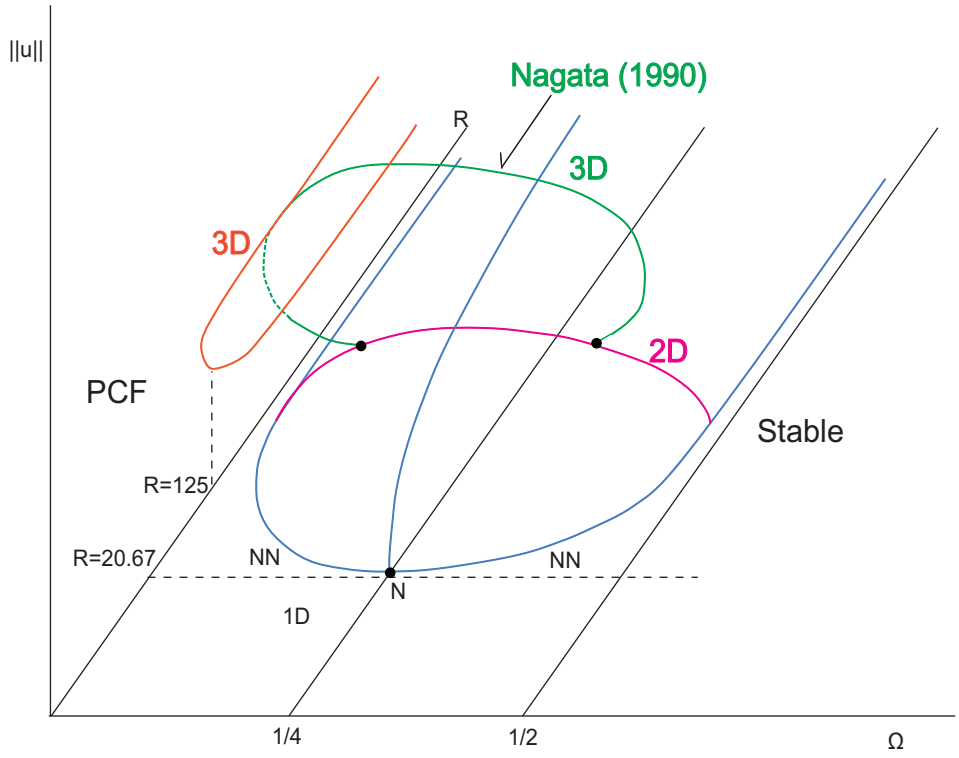

Figure 5: Bifurcation diagram for rotating plane Couette flow.

(relative to a non-dimensionalised shear of 1 across the domain as above). The astrophysical interest is in understanding what hydrodynamic processes can operate in a Keplerian disc which has $\Omega^* \sim R^{-3/2}$ or $\Omega = 2/3$ so as to enhance dissipative processes (see [2] for an introduction to the issues). However, the Rayleigh [10] (axisymmetric) stability criterion predicts that profiles with angular momentum increasing radially outwards i.e. $d(R^2\Omega^*)/dR > 0$ or $\Omega > 1/2$ are stable. This does not preclude non-axisymmetric (streamwise-dependent) instabilities or the existence of disconnected nonlinear solutions as in the plane Couette problem but these have yet to be found (e.g. [7, 16, 14] and [3] for a recent commentary).

References

[1] C. D. Anderek, S. S. Liu, and H. L. Swinney, *Flow regimes in a circular Couette system with independently rotating cylinders*, J. Fluid Mech., 164 (1986), pp. 155–183.

[2] S. A. Balbus, *Spinning discs in the lab*, Nature, 444 (2006), pp. 281–282.

[3] ——, *A turbulent matter*, Nature, 470 (2011), pp. 475–476.

[4] F. H. Busse, *Bounds on the transport of mass and momentum by turbulent flow between parallel plates*, Z. Angew. Math. Phys., 20 (1969), pp. 1–14.

[5] O. Dauchot and F. Daviaud, *Finite-amplitude perturbation and spots growth-mechanism in plane Couette flow*, Phys. Fluids, 7 (1995), pp. 335–343.

[6] P. G. Drazin, *Introduction to Hydrodynamic Stability*, Cambridge University Press, second ed., 2002.

[7] H. Ji, M. Burin, E. Schartman, and J. Goodman, *Hydrodynamic turbulence cannot transport angular momentum effectively in astrophysical disks*, Nature, 444 (2006), pp. 343–346.

[8] D. Joseph, *Nonlinear stability of the Boussinesq equations by the method of energy*, Arch. Rat. Mech. Anal., 22 (1966), pp. 163–184.

[9] D. D. Joseph and S. Carmi, *Stability of Poiseuille flow in pipes, annuli and channels*, Quart. Appl. Math., 26 (1969), pp. 575–599.

[10] Lord Rayleigh, *On the dynamics of revolving fluids*, Proc. R. Soc. Lond. A, 93 (1917), pp. 148–154.

[11] T. Mullin, *Experimental studies of transition to turbulence in a pipe*, Ann. Rev. Fluid Mech., 43 (2011), pp. 1–24.

[12] M. Nagata, *Three-dimensional finite-amplitude solutions in plane Couette flow: bifurcation from infinity*, J. Fluid Mech., 217 (1990), pp. 519–527.

[13] S. A. Orszag, *Accurate solution of the Orr-Sommerfeld stability equation*, J . Fluid Mech., 50 (1971), pp. 659–703.

[14] M. S. Paoletti and D. P. Lathrop, *Angular momentum transport in turbulent flow between independently rotating cylinders*, Phys. Rev. Lett., 106 (2011), p. 024501.

[15] C. C. T. Pringle and R. R. Kerswell, *Asymmetric, helical and mirror-symmetric travelling waves in pipe flow*, Phys. Rev. Lett., 99 (2007), p. 074502.

[16] F. Rincon, G. I. Ogilvie, and C. Cossu, *On the self-sustaining processes in Rayleigh-stable rotating plane Couette flows and subcritical transition to turbulence in accretion disks*, Astron. & Astrophys., 463 (2007), pp. 817–832.

[17] V. A. Romanov, *Stability of plane Couette flow*, Funkcional Anal. i Prolozen, 7 (1973).

[18] B. L. Rozhdestvensky and I. N. Simakin, *Secondary flows in a plane channel: their relationship and comparison with turbulent flows*, J. Fluid Mech., 147 (1984), pp. 261–289.

[19] P. J. Schmid and D. S. Henningson, *Stability and Transition in Shear Flows*, Springer, first ed., 2001.

[20] F. Waleffe, *Homotopy of exact coherent structures in plane shear flows*, Phys. Fluids, 15 (2003), pp. 1–18.